

Coupling of theta activity and glucose metabolism in the human rostral anterior cingulate cortex: An EEG/PET study of normal and depressed subjects

DIEGO A. PIZZAGALLI,^a TERRENCE R. OAKES,^b AND RICHARD J. DAVIDSON^{b,c,d}

^a Department of Psychology, Harvard University, Cambridge, Massachusetts, USA

^b W.M. Keck Laboratory for Functional Brain Imaging and Behavior, University of Wisconsin, Madison, Wisconsin, USA

^c Department of Psychology, University of Wisconsin, Madison, Wisconsin, USA

^d Department of Psychiatry, University of Wisconsin, Madison, Wisconsin, USA

Abstract

In rodents, theta rhythm has been linked to the hippocampal formation, as well as other regions, including the anterior cingulate cortex (ACC). To test the role of the ACC in theta rhythm, concurrent measurements of brain electrical activity (EEG) and glucose metabolism (PET) were performed in 29 subjects at baseline. EEG data were analyzed with a source localization technique that enabled voxelwise correlations of EEG and PET data. For theta, but not other bands, the rostral ACC (Brodmann areas 24/32) was the largest cluster with positive correlations between current density and glucose metabolism. Positive correlations were also found in right fronto-temporal regions. In control but not depressed subjects, theta within ACC and prefrontal/orbitofrontal regions was positively correlated. The results reveal a link between theta and cerebral metabolism in the ACC as well as disruption of functional connectivity within frontocingulate pathways in depression.

Descriptors: Anterior cingulate cortex, Limbic system, Theta rhythm, Positron emission tomography, Electroencephalogram, Source localization

Following the initial description by Jung and Kornmüller (1938), much progress has been achieved regarding the study of neuronal generation of theta activity. Although most nonhuman studies have focused on the septo-hippocampal system, theta has been recorded in numerous other regions, including the anterior cingulate cortex (ACC), entorhinal cortex, hypothalamus, superior colliculus, medial septum, mammillary bodies, anterior thalamus, and amygdala (Bland & Oddie, 1998; Vinogradova, 1995). Theta activity may serve as a gating function on the information processing flow in limbic regions, as some evidence

suggests it facilitates transmission between different structures (Vinogradova, 1995).

In humans, two different manifestations of theta rhythm have been described (Schacter, 1977). The first exhibits a widespread scalp distribution and has been associated with decreased alertness and impaired information processing, typically during drowsy states. The second is associated with a frontal midline distribution and has been linked to alert states characterized by focused attention, mental effort, and effective stimulus processing. Recent human studies have further suggested that either medial prefrontal cortex (PFC) sources centered on the ACC (Asada, Fukuda, Tsunoda, Yamaguchi, & Tonoike, 1999; Gevins, Smith, McEvoy, & Yu, 1997; Ishii et al., 1999), or sources in dorsolateral prefrontal regions (Sasaki et al., 1996) could account for scalp-recorded frontal midline theta activity. These results concur with animal data suggesting that theta associated with alert states arises locally within the ACC and not via volume conduction from the hippocampus (Feenstra & Holsheimer, 1979; Holsheimer, 1982).

Indirect evidence that the human ACC may be involved in the generation of frontal midline theta activity accrues from a comparison of the electrophysiological (EEG/MEG) and hemodynamic neuroimaging literature. In particular, focused attention (hemodynamic: Davis, Taylor, Crawley, Wood, & Mikulis, 1997; EEG: Asada et al., 1999), task difficulty (hemodynamic: Murtha, Chertkow, Beauregard, Dixon, & Evans,

This work was supported by NIMH grants (MH40747, P50-MH52354, MH43454) and by an NIMH Research Scientist Award (K05-MH00875) to Richard J. Davidson. Diego A. Pizzagalli was supported by grants from the Swiss National Research Foundation (81ZH-52864) and "Holderbank"-Stiftung zur Förderung der wissenschaftlichen Fortbildung. We thank Christine L. Larson, Stacey M. Schaefer, Heather C. Abercrombie, and Ruth M. Benca for contributions at early stages of this research; Kathryn A. Horras, Andrew M. Hendrick, and Megan Zuelsdorff for assistance; John Koger for computer support; and Wil Irwin and Alexander J. Shackman for invaluable comments on the manuscript.

Address reprint requests to: Richard J. Davidson, W.M. Keck Laboratory for Functional Brain Imaging and Behavior, University of Wisconsin, 1500 Highland Avenue, Madison, WI 53705-2280, USA. E-mail: rjdavids@facstaff.wisc.edu.

1996; EEG: Gevins et al., 1997), memory load (hemodynamic: Jansma, Ramsey, Coppola, & Kahn, 2000; MEG: Tesche & Karhu, 2000), orienting response (hemodynamic: Williams et al., 2000; EEG: Dietl, Dirlich, Vogl, Lechner, & Strian, 1999), affective processing (hemodynamic: Adinoff et al., 2001; EEG: Aftanas & Golocheikine, 2001), and regulation of the autonomic nervous system (hemodynamic: Critchley, Corfield, Chandler, Mathias, & Dolan, 2000; EEG: Kubota et al., 2001) have been independently associated with ACC activation and frontal midline theta rhythm. Despite this evidence, the relation between hemodynamic/metabolic and electrical activity in the human ACC is unknown, particularly because these studies have not recorded electrophysiological and hemodynamic data simultaneously.

In the above-mentioned and other functional neuroimaging studies, ACC activation was often accompanied by activation in frontal regions, particularly in the dorsolateral PFC. Consistent with this observation, a recent review of 107 PET studies revealed that activations in the superior frontal gyrus and middle frontal gyrus, for example, were significantly more frequent in tasks evoking ACC activation than in those without ACC activation (Koski & Paus, 2000). Because these concomitant activations were observed independently of stimulus modality, channel of response, and over a variety of tasks, they have been interpreted as indices of frontocingulate connections in the human brain, consistent with anatomical evidence suggesting that the dorsolateral PFC sends to and receives dense projections from the ACC, particularly Brodmann area 24 and rostral area 32 (Barbas, 1992; Petrides & Pandya, 1999). In light of the hypothesized role of the ACC in theta activity, it is plausible to expect that frontocingulate connections may become evident in the theta frequency range. Moreover, because frontocingulate pathways have been postulated to play a critical role in the pathophysiology of depression (e.g., Davidson, Pizzagalli, Nitschke, & Putman, 2002; Mayberg, 1997), functional connectivity between the ACC and frontal regions may be disrupted in subjects suffering from major depression.

In the human brain, neuronal activity can be monitored using positron emission tomography (PET) with a modification of the 2-deoxyglucose method originally developed by Sokoloff et al. (1977), using [^{18}F]-2-fluoro-2-deoxy-D-glucose (FDG). Early studies reported direct (Sokoloff, 1989) or indirect (Phelps et al., 1981) evidence for a tight coupling between neuronal activity and energy metabolism, with increasing neuronal activity being associated with increased glucose utilization. Because glucose utilization reflects synaptic (particularly, presynaptic) activity (Jueptner & Weiller, 1995) and scalp EEG signals reflect current associated with excitatory and inhibitory postsynaptic potentials (Nunez & Silberstein, 2000), a link between the two modalities is expected.

Although many EEG/MEG studies have described task-related changes in frontal midline theta, to date none have investigated the link between such activity and metabolism in the ACC during task or baseline recording, nor the relations between theta activity in the ACC and frontal regions, or whether putative functional connectivity within frontocingulate pathways may be disrupted in major depression. The present, methodologically oriented investigation aims to investigate these three topics. To this end, concurrent measurements of brain electrical activity and glucose metabolism were performed in a heterogeneous sample comprised of healthy control and depressed subjects during standard baseline (resting) recording

conditions.¹ The use of a tomographic source localization technique for the EEG data based on realistic head geometry and probabilistic brain atlases enabled the comparison between brain electrical and metabolic activity on a voxelwise basis. Based on the literature reviewed above, a positive association between theta electrical and metabolic activity in the ACC as well as between theta activity in the ACC and dorsolateral PFC were hypothesized. Also, in light of hypothesized dysfunctions in frontocingulate networks in depression, a disruption in functional connectivity between ACC and dorsolateral PFC was expected in subjects suffering from major depression.

Methods

Participants

Participants were recruited through advertisements in local media for a larger study investigating the functional neuroanatomy of major depression (Abercrombie et al., 1998; Pizzagalli et al., 2001). For the present analysis, all participants with both EEG and PET data were included: 17 participants with major depression (mean age: 33.3 years, *SD*: 10.5; 7 women), and 12 control subjects (35.2 ± 11.7 ; 6 women). Based on the *Structured Clinical Interview for the DSM-III-R, Patient Edition* (SCID-P; Spitzer et al., 1992), which was modified to make *Diagnostic and Statistical Manual for Mental Disorders* (DSM-IV) diagnoses, depressed subjects met DSM-IV criteria for major depressive disorder (American Psychiatric Association, 1994), and had no history of mania, psychosis, or other Axis I disorders, with the exception of specific phobias and social phobia secondary to major depressive disorder. Additionally, a family history of mania or psychosis led to study exclusion. For the depressed participants, the mean Beck Depression Inventory (BDI; Beck, Ward, Mendelsen, Mock, & Erbaugh, 1961) and Hamilton Depression Rating Scale (HDRS; 17-item version; Hamilton, 1960) scores were 30.13 (*SD*: 6.79) and 19.0 (*SD*: 5.39), respectively. According to the BDI, 8 of the patients were "severely depressed" ($\text{BDI} > 30$), and 8 were "mild/moderately depressed" ($13 < \text{BDI} < 29$; Beck & Steer, 1987). Control participants had no current or past Axis I pathology in themselves or first-degree relatives. Additional details about participant recruitment, assessment, and characteristics have been reported elsewhere (Pizzagalli et al., 2001).

Procedure

After obtaining written informed consent, participants underwent concurrent FDG-PET and EEG recording, following a protocol approved by the Human Subjects Committee of the University of Wisconsin. Injection of FDG was scheduled between 11:00 and 13:30 hr. Participants fasted for 5 hr prior to the injection. After application of scalp EEG electrodes, two 22-gauge intravenous catheters (injection and blood draw) were inserted for the PET procedure, one in the antecubital fossa of the right arm and the other in a vein in the posterior aspect of the left hand. To allow rapid sequential sampling of arterialized venous blood, the left hand was placed into a heated handwarmer

¹The inclusion of both healthy control and depressed subjects likely led to a larger range of ACC activation, as depression has been associated with dysfunctional activity in the ACC (for review, see Davidson et al., 2002). A potentially large range of ACC activation appeared optimal for the correlational approach used in the current study.

(Phelps et al., 1979); the right hand was also heated to equate thermal stimulation on both sides. Participants were instructed to remain still, sit quietly, and relax but stay awake during uptake. To obtain an initial plasma glucose level, a 1- to 2-ml blood sample was drawn. Subsequently, approximately 5 milliCuries (range: 3.8–5.7 mCi) of FDG were administered by means of a bolus injection into the intravenous line in the right arm. Arterialized blood samples were drawn from the left hand throughout the 30 min following injection. Each blood sample was centrifuged, 0.5 ml of plasma was withdrawn, and the radioactivity level was measured in a well counter to obtain the blood time course of radioactivity.

EEG recording consisted of 10 contiguous 3-min trials (5 with eyes open and 5 with eyes closed, alternating according to a counterbalanced order across participants) covering the 30 min required for radiotracer injection and uptake. Consequently, the EEG and PET data reflect the same functional brain state. Alternation of eyes open and eyes closed trials was selected as previous studies from our laboratory (Tomarken, Davidson, Wheeler, & Kinney, 1992) have suggested that aggregating across eyes open and eyes closed trials results in the most reliable estimates of baseline EEG activation patterns. Following a 10-min break in which participants were encouraged to void their bladders, participants were positioned on the PET scanner.

Apparatus and Physiological Recording

EEG data. Twenty-eight-channel EEG was recorded referenced to the left ear with a modified lycra electrode cap (Electro-Cap International, Inc.). Horizontal and vertical electrooculogram (EOG) channels were also recorded. Impedances were below 5 K Ω (EEG) and 20 K Ω (EOG). Signals were amplified with a Grass Model 12 Neurodata system using Model 12C preamplifiers (bandpass: 1–300 Hz; 60-Hz Notch filter), filtered with MF6 digital anti-aliasing low-pass filters set at 100 Hz, and digitized at 250 Hz.

PET data. [^{18}F]-fluoride was produced by a CTI RDS Cyclotron (Knoxville, TN, USA), and FDG was synthesized using the modified method of Hamacher (Hamacher, Coenen, & Stocklin, 1986). A General Electric/Advance PET scanner (Milwaukee, WI, USA) was used to acquire PET data (intrinsic in-plane and axial resolutions of approximately 5 mm full-width half-maximum [FWHM]). The PET scan started approximately 50 min after injection and consisted of a 30-min two-dimensional emission scan (15.2-cm field of view, 35 transaxial planes), a 10-min three-dimensional emission scan, and a 10-min transmission scan.

Data Reduction and Analyses

EEG data. Off-line, data were screened for artifacts caused by blinks, eye movements, muscle activity, or technical problems. Only epochs with artifact-free data across all channels were considered for the analyses. All available artifact-free 2,048-ms EEG epochs from both the eyes open and eyes closed trials were extracted (150.83 ± 73.22 vs. 168.21 ± 83.98 , respectively, with no differences between eyes open and eyes closed trials, $t_{28} = 0.82$, n.s.), rederived to the average reference, and then subjected to standard spectral analyses via Discrete Fourier Transform (DFT) using a boxcar windowing (Brillinger, 1981). Subsequently, the three-dimensional intracerebral current density distribution for the theta band (6.5–8.0 Hz) was estimated

using Low Resolution Electromagnetic Tomography (LORETA; Pascual-Marqui, Michel, & Lehmann, 1994; Pascual-Marqui et al., 1999). This technique has recently received important cross-modal validation, as summarized elsewhere (Pizzagalli et al., 2001). Without postulating a prespecified number of generating sources, LORETA estimates location(s) of electrical source activity by assuming similar activation among neighboring neuronal sources, an assumption implemented by computing the “smoothest” of all possible activity distributions. The present implementation uses a three-shell spherical head model (Ary, Klein, & Fender, 1981) and EEG electrode coordinates derived from cross-registrations between spherical and realistic head geometry (Towle et al., 1993). Both the head model and the electrode coordinates were registered to the digitized MRI available from the Brain Imaging Centre, Montreal Neurologic Institute (MNI305; Collins, Neelin, Peters, & Evans, 1994; Evans et al., 1993). The solution space (2,394 voxels; voxel size: $7 \times 7 \times 7 \text{ mm}^3$) was restricted to cortical gray matter and hippocampi, as defined by the digitized MNI probability atlases. Consequently, all coordinates reported in the present study are in MNI space. Subsequently, the Structure–Probability Maps atlas (Lancaster et al., 1997) was used to label gyri and Brodmann area(s). Because the Structure–Probability Maps atlas requires Talairach coordinates, and due to the imperfect match between the MNI and Talairach templates, MNI coordinates were converted to Talairach coordinates (Talairach & Tournoux, 1988) using the corrections proposed by Brett, Johsrude, and Owen (2002; see also <http://www.mrc-cbu.cam.ac.uk/Imaging/mninspace.html>).

LORETA values represent the power, that is, squared magnitude, of the computed intracerebral current density (unit: amperes per square meter, A/m^2).

PET data. Using the scanner manufacturer’s software (General Electric, Milwaukee, WI, USA), the two-dimensional PET data were reconstructed with calculated attenuation correction to $1.17 \times 1.17 \times 4.25 \text{ mm}^3$ voxels, and converted to parametric images of an influx constant (K_i , 1/s) using the measured radioactive blood time course and a variation of the Sokoloff method (Phelps et al., 1979). They were then spatially normalized with SPM99 (Friston, Worsley, Frackowiak, Mazziotta, & Evans, 1994) to the template used by LORETA (MNI305), converted to $2 \times 2 \times 2 \text{ mm}^3$ voxels, and smoothed with a $6 \times 6 \times 6 \text{ mm}^3$ Gaussian kernel to match the estimated resolution of LORETA ($\sim 10 \text{ mm}^3$). Using in-house software that considered weighting factors derived from the fractional volume of a PET voxel within a given LORETA voxel, PET data were resampled to voxels having the same size and center location as the LORETA voxels (Oakes et al., 2001). PET data are expressed in units of $\mu\text{g}/\text{min}/100 \text{ cc}$.

Statistical Analyses

Voxelwise correlation analyses. Two sets of data were analyzed. In the first approach, which emphasizes subject-to-subject global variations in activation, neither the LORETA nor the PET data were intensity normalized. In the second approach, subject-to-subject global variations were removed in both LORETA and PET data by intensity normalization. The average value across voxels for each subject’s volume was computed, and then each image volume was scaled so its mean was the same as the overall mean. This approach emphasizes regional differences within the brain. At each voxel, a correlation was computed

between current density for the theta band and glucose metabolism for both normalized and nonnormalized data. Due to different distributions of the LORETA and PET data, Spearman's rank correlations (ρ) were computed.

Region-of-interest analysis. In addition to the whole-brain correlational analyses, a region-of-interest (ROI) analysis was performed. In a recent EEG study, we found that theta activity in a rostral ACC cluster was specifically associated with favorable treatment response in depression (Pizzagalli et al., 2001). In that study, this association was postulated because (a) metabolic rate in the rostral ACC had been previously associated with treatment response in PET studies (Mayberg et al., 1997), and (b) the ACC had been proposed as a possible neuronal source of theta activity in the human brain (Asada et al., 1999; Gevins et al., 1997; Ishii et al., 1999). In the present analysis, LORETA and PET activity was averaged from the rostral ACC cluster differentiating low and high treatment responders (Figure 1C). For both normalized

and nonnormalized data, Spearman's rank correlations assessed the relation between the ROI values of the two modalities.

Functional connectivity analyses. To test the role of theta activity on other regions, Spearman's rank correlations were computed between theta activity in the ACC and other regions showing significant positive correlations between the EEG and PET data (see Results). For each pair of regions, Fisher's tests for independent correlations (Fisher, 1921) were run to assess whether these patterns of correlations were similar for depressed and control subjects.

In addition, to investigate in more detail whether depression may be associated with dysregulation in frontocingulate networks, the functional connectivity between the ACC and the rest of the brain was interrogated for depressed and control subjects separately. To this end, Spearman's rank correlations were run between theta current density within the ACC (averaged within cluster #1, Figure 2; see Results) and each voxel in the LORETA brain volume. Again, to test whether depressed and control

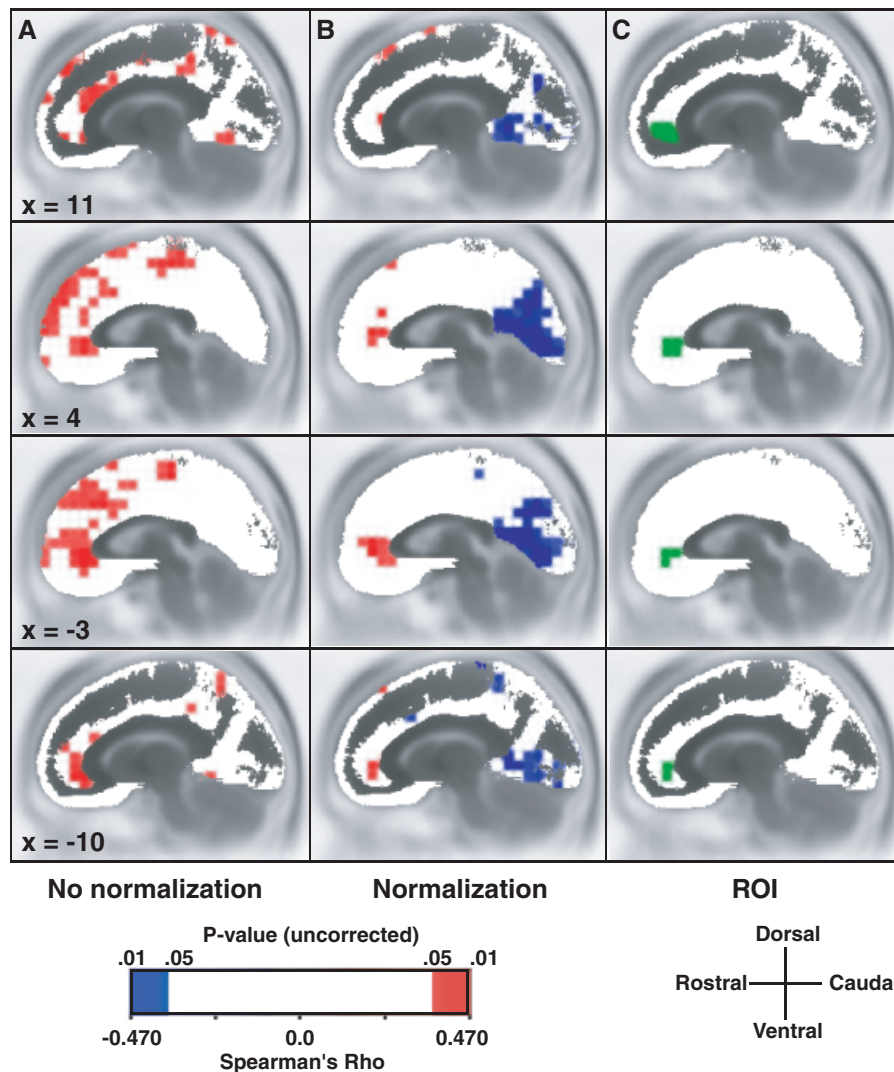


Figure 1. Sagittal slices centered on the ACC showing results of voxelwise Spearman's rank correlation between current density in the theta band (6.5–8.0 Hz) and glucose metabolism in 29 subjects using (A) nonnormalized data and (B) normalized data. For display purposes only, maps have been thresholded at $p < .05$ (uncorrected). C: Location and spatial extent of the rostral ACC region (see green) previously found to be associated with treatment response in major depression (Pizzagalli et al., 2001).

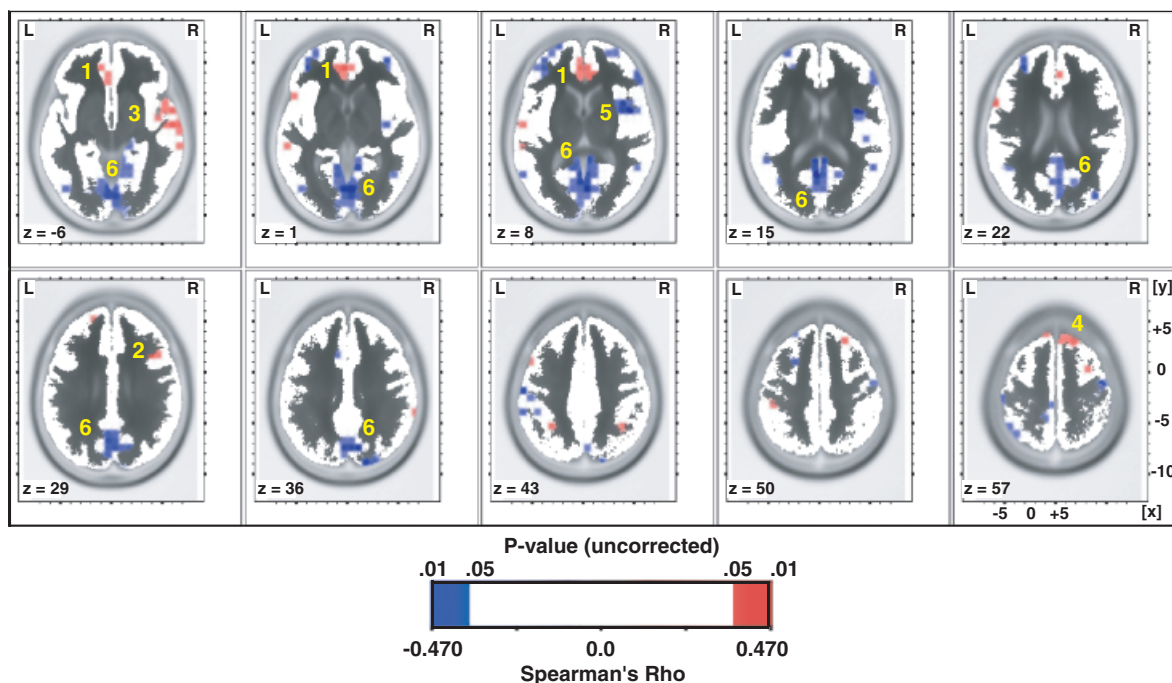


Figure 2. Axial slices (head seen from above, nose up, L = left, R = right) showing thresholded results of voxelwise Spearman's rank correlation between current density for the theta band (6.5–8.0 Hz) and glucose metabolism in 29 subjects. For display purposes only, maps have been thresholded at $p < .05$ (uncorrected). Cluster #1: anterior cingulate cortex; cluster #2: right middle frontal gyrus; cluster #3: right middle and superior temporal gyri; cluster #4: right superior frontal gyrus; cluster #5: right precentral gyrus; cluster #6: cuneus, precuneus, culmen, posterior cingulate, and lingual gyri.

subjects may differ in functional connectivity between the ACC and other regions, Fisher's tests for independent correlations were run at each voxel.

Overall, for regions with a priori hypotheses (e.g., ACC), significant results were accepted at $p < .05$. For regions without a priori hypotheses, a p value of .01 was selected, as previous LORETA studies using randomization procedures to estimate the false-positive rate under the null hypothesis have found that this threshold is adequate for protecting against Type I errors (Pizzagalli et al., 2002).

Results

Voxelwise Correlation Analyses

Nonnormalized LORETA and PET data. Figure 1A shows the results of the whole-brain correlation analysis for the entire sample ($n = 29$) between theta current density and glucose metabolism at each voxel when no normalization was applied to either the EEG or PET data. Out of the 2,394 correlations, 2,317 were positive and 213 of them were significant at $p < .05$. No significant negative correlation emerged. Although positive correlations between theta current density and glucose metabolism were present in the ACC, they were not specific to this region. These data include the global activity for each subject, which is considered to be a nuisance variable; consequently, subsequent analysis focused on the normalized data.

Normalized LORETA and PET data. Figures 1B and 2 and Table 1 summarize the results of the whole-brain correlation analysis for the entire sample ($n = 29$) between theta current

density and glucose metabolism at each voxel when normalization was applied to both the EEG and PET data. A cluster in the rostral ACC (Brodmann areas (BAs) 24, 32) showed the largest (13 voxels, volume: 4.46 cm^3) and second strongest positive correlation between theta current density and glucose metabolism ($\rho = .52$, $p < .005$; $X = -3$, $Y = 45$, $Z = 1$; BA 32; see cluster #1, Figure 2). The strongest positive correlation was observed in the right middle frontal gyrus ($\rho = .54$, $p < .0025$; $X = 39$, $Y = 17$, $Z = 29$; BA 9; see cluster #2, Figure 2), in a cluster that was, however, comprised of only 2 voxels (0.69 cm^3). As listed in Table 1, only two further clusters showed reliable positive correlations, one involving the right middle and superior temporal gyri ($\rho = .50$, $p < .01$; 11 voxels, 3.77 cm^3 ; see cluster #3, Figure 2) and the other the right superior frontal gyrus ($\rho = .48$, $p < .01$; 4 voxels, 1.37 cm^3 ; see cluster #4, Figure 2). For each of these clusters, the highest correlation was associated with a p value smaller than .01, suggesting adequate protection against Type I errors. The strongest negative correlation was observed in the right precentral gyrus ($\rho = -.67$, $p < .0001$; $X = 46$, $Y = 3$, $Z = 8$; BA 44; 4 voxels, 1.37 cm^3 ; see cluster #5, Figure 2), whereas the largest cluster with negative correlations encompassed the cuneus, precuneus, culmen, posterior cingulate and lingual gyri (78 voxels, 26.75 cm^3 ; BAs 18, 19, 23, 29, 31; see cluster #6, Figure 2).

Region-of-Interest Analysis

As shown in Figure 1C, the rostral ACC cluster (14 voxels, 4.80 cm^3) previously found to be associated with treatment response in depression (Pizzagalli et al., 2001) overlapped with the region with the reliable positive correlations between LORETA and PET data (Figure 1B). For both the normalized

Table 1. Summary of Significant Positive Spearman's Rank Correlations between Theta Current Density and Glucose Metabolism ($n = 29$)

Region (cluster in Figure 2)	BA	Side	No. voxels	Spearman ρ	X	Y	Z
Anterior cingulate (#1)	24/32	Right	5	.433 ± .03	5.8 ± 3.5	41.5 ± 4.0	6.3 ± 3.5
		Left	8	.418 ± .05 ^a	-4.8 ± 3.2	40.6 ± 5.2	0.1 ± 5.8
Middle frontal gyrus (#2)	6	Right	2	.473 ± .09 ^a	42.5 ± 4.9	17.0 ± 0.0	29.0 ± 0.0
		Left	—	—	—	—	—
Middle temporal gyrus (#3)	21	Right	7	.426 ± .04 ^a	61.0 ± 6.3	-11.0 ± 12.1	-8.0 ± 3.4
		Left	—	—	—	—	—
Superior temporal gyrus (#3)	22	Right	4	.422 ± .03	53.0 ± 5.7	3.0 ± 5.7	6.0 ± 0.0
		Left	2	.410 ± .01	-59.0 ± 0.0	-21.5 ± 14.8	8.0 ± 0.0
Superior frontal gyrus (#4)	6	Right	4	.421 ± .03 ^a	14.5 ± 9.0	31.0 ± 0.0	55.3 ± 3.5
		Left	—	—	—	—	—

The mean ($\pm SD$) coordinates and mean ($\pm SD$) correlation of clusters showing significant positive Spearman's rank correlations (ρ) are listed. Note that these correlations differ from the one reported in the main text, where the highest correlation within a given cluster is provided. The spatial extent (number of voxels exceeding the $p < .05$, uncorrected, $n = 29$), hemisphere, and Brodmann areas of these clusters are also provided. Coordinates in millimeters (MNI space), origin at anterior commissure; (X) = left (-) to right (+); (Y) = posterior (-) to anterior (+); (Z) = inferior (-) to superior (+).

^aHighest correlation within the cluster is associated with $p < .01$, Spearman $\rho > .475$.

($\rho = .34$, $n = 29$, $p = .067$) and the nonnormalized ($\rho = .44$, $n = 29$, $p < .025$) data, a positive correlation emerged.

Highlighting the specificity of a link between theta activity and glucose metabolism in the rostral ACC, no reliable correlations emerged for control or depressed subjects, or for the entire sample, when repeating the ROI analyses for other frequency bands, such as delta (1.5–6.0 Hz), alpha1 (8.5–10.0 Hz), alpha2 (10.5–12.0 Hz), beta1 (12.5–18.0 Hz), beta2 (18.5–21.0 Hz), beta3 (21.5–30.0 Hz), and gamma (36.5–44 Hz), all p 's $> .05$.

Functional Connectivity Analyses

To test the role of theta activity in the ACC on other regions showing significant positive correlations between the EEG and PET data, Spearman's rank correlations were computed between theta activity in the ACC, on one hand, and in the right middle frontal gyrus (cluster #2, Figure 2), right middle and superior temporal gyri (cluster #3, Figure 2), and the right superior frontal gyrus (cluster #4, Figure 2), on the other hand. ACC theta activity was significantly correlated with theta activity in the right superior frontal gyrus ($\rho = .66$, $n = 29$, $p < .001$) and right middle temporal gyrus ($\rho = -.38$, $n = 29$, $p < .05$), but not with theta activity in the right superior temporal ($\rho = -.32$, n.s.) or right middle frontal ($\rho = .30$, n.s.) gyri. These patterns of correlations were similar for depressed ($n = 17$) and control ($n = 12$) subjects, with one exception. Whereas the correlations for the right middle frontal gyrus (.19 vs. .52), right middle (-.49 vs. -.16), and superior temporal gyri (-.33 vs. -.13) did not differ between depressed and control subjects, those for the right superior frontal gyrus were significantly different (.37 vs. .89, $z = -2.39$, $p < .02$), as assessed with Fisher's test for independent correlations. Thus, compared to controls, depressed subjects showed significantly lower functional connectivity between the ACC and the right superior frontal gyrus.

Spearman's rank correlations were run between theta current density within the ACC (averaged within cluster #1, Figure 2) and each voxel in the brain volume to examine putative dysregulation involving the ACC in depression. As evident in Figure 3A, control subjects showed significant correlations ($p < .01$) between the ACC and various regions in the prefrontal and orbitofrontal cortex, such as the inferior (BAs 11/47), middle (BAs 8/9/11), superior (BAs 8/9/10/11), and medial (BAs 6/8/9/

10/11) frontal gyrus, as well as the orbital gyrus (BA 11).² In control subjects, most of these significant correlations were located in the right hemisphere (Figure 3A). To test whether this laterality effect was statistically supported, the formula proposed by Meng, Rosenthal, and Rubin (1992) was used to assess whether the correlations between the ACC and right-sided regions were significantly different from the correlations between the ACC and left-sided regions. Right-sided regions were defined as follows: first, left-sided regions displaying significant correlations were flipped by reversing the X coordinates (Pizzagalli et al., 2002); second, those flipped left-sided regions were subtracted from right-sided regions showing significant correlations to eliminate spatial overlap between regions in the two hemispheres with significant correlations. Subsequently, this spatially unique cluster was projected back to the left hemisphere. Finally, for both clusters, correlations were averaged and entered in the formula proposed by Meng et al. (1992; see p. 173). Among the four separate clusters tested, only the OFC cluster (see yellow circle in Fig. 3A) showed significantly higher correlations than the homologous region in the left hemisphere ($\rho_{\text{ACC-right OFC}} = .83$, $p < .01$; $\rho_{\text{ACC-left OFC}} = .49$, n.s.; $Z = 2.66$, $n = 12$, $p < .02$; note: $\rho_{\text{right OFC-left OFC}} = .85$, $p < .01$).

Depressed subjects, on the other hand, were characterized by significant correlations that were restricted to more medial regions (Figure 3B). Voxel-by-voxel Fisher's tests confirmed that the correlations between the ACC, on one side, and right dorsolateral PFC, ventrolateral PFC, and orbitofrontal cortex, on the other side, were significantly lower for depressed than control subjects (Table 2). Notably, apart from a single voxel in the inferior occipital gyrus ($X = 39$, $Y = -88$, $Z = -13$; BA 18) at which depressed subjects showed significantly higher correlations than controls ($z = 1.99$, $p < .05$), significant differences between control and depressed subjects were restricted to anterior regions of the brain ($Y > 31$) that involved the dorsolateral PFC and orbitofrontal cortex. A closer look at

²In these analyses correlating theta activity averaged within a subregion of the ACC (see cluster #1, Figure 2) with the rest of the brain, significant results involving the ACC should not be further considered. Due to the redundancy of these data and the smoothness assumption implemented in the LORETA algorithm, neighboring voxels in the ACC are highly correlated, which led to inflated correlations.

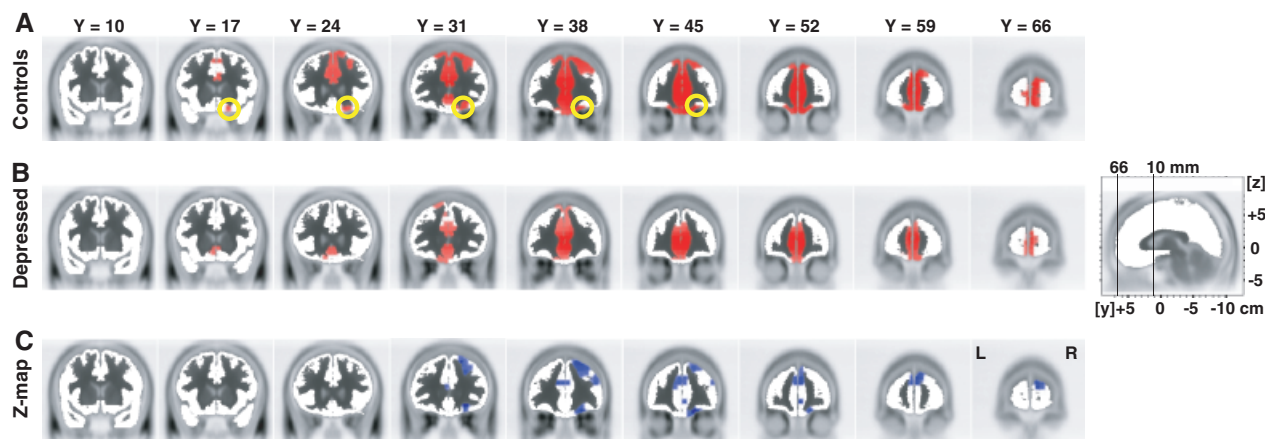


Figure 3. Coronal slices (L = left, R = right) showing thresholded results of voxelwise Spearman’s rank correlation between current density for the theta band (6.5–8.0 Hz) within the ACC (averaged within cluster #1 from Figure 2) and each voxel in the brain volume for (A) control subjects and (B) depressed subjects. Maps thresholded at $p < .01$ (uncorrected); red colors denote positive correlations. In C, significant results of Fisher’s test for independent correlations between depressed and control subjects are displayed. Z maps thresholded at $p < .05$ (uncorrected); blue colors denote significantly lower correlations for depressed than control subjects. In A, the yellow circle denotes voxels in the right OFC in which control subjects had significantly higher correlations between the rostral ACC and the right OFC than correlations between the rostral ACC and homologous, left-sided regions, as assessed by the formula proposed by Meng et al. (1992).

Figure 3 reveals again that group differences in correlations between the ACC and PFC/OFC regions were predominantly restricted to the right hemisphere. To formally test whether this laterality effect was statistically supported, we extracted z values from voxels in the left hemisphere that were homologous to the ones listed in Table 2 (by reversing the X coordinates). Subsequently, z values at right- and left-sided clusters were tested by using the formula proposed by Rosenthal (1987; p. 182), $Z' = [(Z_{\text{right}} - Z_{\text{left}})/\sqrt{2}]$. No significant differences emerged (all $|z| < 1.30$, n.s.), suggesting that the differences between depressed and control subjects in correlations between the ACC and right-sided regions were not significantly different from the differences between depressed and control subjects in correlations between the ACC and left-sided regions.

Discussion

Using an analytic approach involving a distributed source localization technique for EEG data based on realistic head geometry and probabilistic brain atlases, we found positive correlations between theta current density and glucose metabolism in rostral regions of the ACC (BAs 24, 32), as well as in right

fronto-temporal regions, including the right middle (BA 9) and superior (BA 6) frontal gyri, and the right middle (BA 21) and superior (BA 22) temporal gyri. For the rostral ACC, the association between brain electrical and metabolic activity was absent for other classic EEG bands. Under normal conditions, glucose is the primary source of energy for the brain, and the coupling between neuronal activity and glucose utilization implies that spatially localized and temporally delimited increases in glucose utilization occur in association with neuronal activity in circumscribed brain regions subserving a specific function (Magistretti, 2000; Sokoloff, 1989). Consistent with the notion that neuronal activity leads to localized increases in glucose metabolism, the relations between strength of theta current density and glucose metabolism emerged especially when relative rather than absolute glucose metabolism was considered, where subject-to-subject global variations in both data sets have been removed and thus regional activations have been emphasized. Overall, these results suggest that in the alert resting state, higher cerebral metabolism is associated with greater EEG theta in territories of the human cortex that, on the basis of the animal neurophysiology, are expected to be regulated by limbic theta. Direct or indirect evidence for a critical role of the ACC in the

Table 2. Summary of Significant Differences between Depressed and Control Subjects in Functional Connectivity between the ACC and Various Prefrontal and Orbitofrontal Regions

Region	BA	Side	Z value	X	Y	Z
Superior frontal gyrus	11	Right	- 3.04	18	45	- 20
Inferior frontal gyrus	47	Right	- 2.97	25	31	- 13
Middle frontal gyrus	8	Right	- 2.88	18	31	50
Superior frontal gyrus	11	Right	- 2.71	25	45	- 20
Inferior frontal gyrus	11	Right	- 2.59	25	38	- 20

The coordinates, Brodmann areas, hemisphere, and z values of voxels showing significant differences between depressed and control subjects are listed (all p 's < .01). At each voxel in the brain volume, Fisher’s test for independent correlations were run to assess whether the Spearman’s rank correlations between theta current density within the ACC (averaged within cluster #1, Figure 2) and that voxel differed between depressed and control subjects. Negative z values refer to significantly lower correlations for depressed than control subjects. Coordinates in millimeters (MNI space), origin at anterior commissure; (X) = left (-) to right (+); (Y) = posterior (-) to anterior (+); (Z) = inferior (-) to superior (+).

generation of theta rhythm can be found in prior invasive animal and human research as well as EEG/MEG studies using various source localization techniques. First, in rodents, theta rhythm has been directly recorded from anterior and posterior regions of the cingulate gyrus (Borst, Leung, & MacFabe, 1987; Destrade & Ott, 1982; Feenstra & Holsheimer, 1979; Leung & Borst, 1987). Whereas some studies have suggested that this activity may be caused by volume conduction from other regions (Leung & Borst, 1987), others have reported polarity inversion (which implies theta generation) in the cingulate cortex (Feenstra & Holsheimer, 1979; Holsheimer, 1982). Second, in patients with intracranial recording for epilepsy assessment, electrical stimulation of the ACC (midportion of BA 24) has been found to induce a 3–8 Hz rhythm in frontomedial recordings as well as autonomic changes (Talairach et al., 1973). Similarly, scalp and intracranial ictal recordings in patients with cingulate cortex seizures showed rhythmic frontal theta activity (Devinsky, Morrell, & Vogt, 1995). Third, experimental manipulations involving focused attention, working memory, and regulation of the autonomic nervous system, for example, elicited both ACC activation and frontal midline theta activity (Asada et al., 1999; Davis et al., 1997; Dietl et al., 1999; Gevins et al., 1997; Jansma et al., 2000; Tesche & Karhu, 2000; Williams et al., 2000). Finally, single or distributed sources modeled in medial PFC or dorsal ACC regions have been shown to account for theta activity recorded maximally over frontal midline scalp regions (Asada et al., 1999; Gevins et al., 1997; Ishii et al., 1999). The present results achieved with voxelwise comparisons of concurrently recorded EEG and PET data agree with and extend these findings by showing that tonic ACC activation during task-free resting conditions was associated with current density of theta activity in the same region.

Results from the current data set cannot establish whether theta activity in the ACC relies on intrinsic local properties, patterns of afferent inputs, or passive propagation from brain regions not included in the LORETA solution space. In rodents, theta has been recorded from the hippocampus and entorhinal cortex, but its generation is dependent on the medial septum. Occurrence of hippocampal theta is crucially dependent on afferents from the medial septum/vertical limb of the diagonal band of Broca complex (MS/vDBB), which is considered the pacemaker of hippocampal theta (Vertes & Kocsis, 1997; Vinogradova, 1995). Whereas lesions or pharmacological blockade of the MS/vDBB led to abolition of hippocampal activity, the same was not true for cingulate theta activity (Borst et al., 1987; Destrade & Ott, 1982). Thus, theta can be generated in the cingulate cortex independently of the hippocampal system. Alternatively, because the horizontal limb of the diagonal band projects over the genu of the corpus callosum to the anterior limbic area of the cingulate cortex (BA 24; Swanson & Cowan, 1979), theta in the ACC may be driven by reciprocal anatomical connections with other subcortical areas involved in its generation.³ Despite these anatomical details, the intracellular mechanisms governing theta rhythm in the ACC are unknown. At least in the hippocampus, it seems that inhibitory postsynaptic

potentials are not involved in the generation of theta rhythm but that two excitatory synaptic influences contribute to the intracellular theta rhythm: an acetylcholine-mediated sustained depolarization of septal origin and glutamate-mediated EPSP (Steriade, Gloor, Llinás, Lopes da Silva, & Mesulam, 1990). If these mechanisms extend to the ACC, this would explain the positive relation between electrical and metabolic activity.

Frontocingulate Network and Depression

In the present study, strong positive correlations were found in control subjects between theta current density in the rostral ACC and various regions within the prefrontal and orbitofrontal cortices, particularly in the right hemisphere. Conversely, depressed subjects showed no statistical evidence for such correlations, and, compared to control subjects, were characterized by significantly lower correlations between ACC, on one hand, and right PFC and orbitofrontal regions,⁴ on the other hand. In control subjects, these indices of functional connectivity between the ACC and frontal regions are consistent with anatomical evidence suggesting that the dorsolateral prefrontal and orbitofrontal cortices send to and receive dense projections from the ACC (Barbas, 1992; Petrides & Pandya, 1999), particularly area 24 and rostral area 32. In agreement with these anatomical data, a recent meta-review of 107 PET studies revealed that changes in blood flow in dorsolateral and orbitofrontal cortices were more likely to occur in tasks evoking ACC activation than in those without ACC activation (Koski & Paus, 2000). Moreover, in a recent study, modulations of dorsolateral PFC activation through repetitive transcranial magnetic stimulation (rTMS) to the left mid-dorsolateral PFC were associated with similar blood flow changes in the ACC (Paus, Castro-Alamancos, & Petrides, 2001).

Evidence of disrupted functional connectivity between the ACC and PFC regions in major depression is intriguing. According to an influential theory of ACC function (Botvinick, Braver, Barch, Carter, & Cohen, 2001), the ACC plays a key role in monitoring conflicts among brain regions. In this theory, the ACC serves an evaluative function reflecting the degree of response conflict elicited by a given task. When conflict is detected, the ACC issues a call for further processing to the dorsolateral PFC, which is assumed to be critical for controlled processing and for guiding behavior toward a goal by adjudicating among various response options. Thus, the dorsolateral PFC represents and maintains task demands necessary for such control and modulates neural activity in brain regions implicated in the conflict. Interestingly, the region of the ACC involved in the present study is slightly more rostral compared to the one involved in conflict monitoring, and has been implicated in error detection and emotional evaluation of errors, two further situations requiring executive control of actions (Kiehl, Liddle, & Hopfinger, 2000; Luu, Tucker, Derryberry, Reed, & Poulsen, 2003; Milham et al., 2001). In recent reviews, abnormalities in

³For example, theta may arise in the ACC as a synaptically transferred activity either from the hippocampus to the mammillary bodies and the anterior thalamic nuclei that project to area 24 or from the hippocampus to the entorhinal cortex that projects to many associational cortical areas, including area 24. Unfortunately, the present EEG/PET data do not offer the opportunity to test these hypotheses.

⁴Although these group analyses revealed significant results that were lateralized to the right hemisphere, it is important to stress that a formal test of this putative laterality effect revealed no statistical differences between the right and the homologous voxels in the left hemisphere (see Davidson & Irwin, 1999, for a discussion of the importance of testing laterality effects in neuroimaging studies). Thus, the group differences in correlations between the ACC and right PFC/OFC were not statistically different from the group differences in correlations between the ACC and left PFC/OFC. As a consequence, no further discussion or interpretation of these “laterality” effects is presented.

cross talk between the ACC and PFC have been emphasized in the pathophysiology of depression (Davidson et al., 2002; Mayberg, 1997). By highlighting diminished functional connectivity during task-free resting conditions between the ACC and various prefrontal regions, including the dorsolateral prefrontal and orbitofrontal cortex, the present findings provide initial empirical evidence for this assumption. Whether in depression such abnormalities in functional connectivity reflect ACC-based impairments in conflict monitoring, particularly in the affective evaluation of conflicts and errors, or PFC-based impairments in controlled processing, or both, is currently unclear.

Limitations and Future Directions

Although both cerebral glucose metabolism and neuroelectrical activity reflect synaptic activity, several factors contribute to an ill-posed comparison between the two modalities that limits the interpretation of any EEG-PET analysis. First, EEG signals recorded at the scalp are highly dependent on synchronization/desynchronization mechanisms, and their relation to glucose utilization is unclear (Nunez & Silberstein, 2000). For instance, increased neuronal firing associated with reduced synchrony would lead to a small signal recorded at the scalp, yet it would require substantial glucose supply (e.g., alpha blockade after eye opening). Further, it is well known that both excitation and inhibition require glucose utilization (Ackermann, Finch, Babb, & Engel, 1984). For example, loss of inhibitory synaptic action in specific conditions (e.g., interictal periods in epileptic patients) would lead to large EEG spikes but low metabolic utilization. Second, whereas FDG-PET measures glucose metabolism irrespectively from the spatial arrangement of the activated neurons, scalp EEG cannot detect activity arising from

assemblies arranged in closed electrical fields (Nunez & Silberstein, 2000). This may explain why no reliable correlations were observed in the present study within the hippocampus—the region most commonly investigated in relation to the theta rhythm in nonhuman studies—which, due to its structural features, represents a closed field. Also, spatial configurations involving opposing dipoles located in sulci generate activity that is opaque to scalp EEG recordings, as the dipoles would cancel. Third, coupling of synaptic activity and energy metabolism is assumed to primarily occur in astrocytes (Magistretti, 2000), glial cells with a “closed field” structure that would be, again, electrically invisible. Finally, perhaps the most important limitations of the present study are its correlational nature and the fact that the reported relation between theta activity and regional glucose metabolism pertained to resting-state data only. Although we expect that such results would extend to task-elicited theta, with different subdivisions of the ACC involved (“cognitive” vs. “affective”) depending on the nature of the task (Paus, 2001), future studies using experimental manipulations known to activate the ACC are needed for testing whether such task-induced changes produce systematic variation in both the theta signal and simultaneously measured hemodynamic or metabolic changes in this region. Importantly, due to the correlational nature of the study, the present findings—though not inconsistent with it—cannot provide direct evidence that theta activity is generated in or modulated by the ACC. Despite these limitations, the present study showcases a novel approach to compare metabolic and electrical activity on a voxelwise basis, and suggests functional coupling between theta activity and glucose metabolism in the rostral ACC as well as functional connectivity within frontocingulate networks that appears to be disrupted in major depression.

REFERENCES

- Abercrombie, H. C., Schaefer, S. M., Larson, C. L., Oakes, T. R., Holden, J. E., Perlman, S. B., Krahn, D. D., Benca, R. M., & Davidson, R. J. (1998). Metabolic rate in the right amygdala predicts negative affect in depressed patients. *NeuroReport*, *9*, 3301–3307.
- Ackermann, R. F., Finch, D. M., Babb, T. L., & Engel, J., Jr. (1984). Increased glucose metabolism during long-duration recurrent inhibition of hippocampal pyramidal cells. *Journal of Neuroscience*, *4*, 251–264.
- Adinoff, B., Devous, M. D., Best, S. M., George, M. S., Alexander, D., & Payne, K. (2001). Limbic responsiveness to procaine in cocaine-addicted subjects. *American Journal of Psychiatry*, *158*, 390–398.
- Aftanas, L. I., & Golocheikine, S. A. (2001). Human anterior and frontal midline theta and lower alpha reflect emotionally positive state and internalized attention: High-resolution EEG investigation of meditation. *Neuroscience Letters*, *310*, 57–60.
- American Psychiatric Association. (1994). *Diagnostic and statistical manual for mental disorders* (4th ed.). Washington, DC: American Psychiatric Press.
- Ary, J. P., Klein, S. A., & Fender, D. H. (1981). Location of sources of evoked scalp potentials: Corrections for skull and scalp thicknesses. *IEEE Transactions on Biomedical Engineering*, *28*, 447–452.
- Asada, H., Fukuda, Y., Tsunoda, S., Yamaguchi, M., & Tonoike, M. (1999). Frontal midline theta rhythms reflect alternative activation of prefrontal cortex and anterior cingulate cortex in humans. *Neuroscience Letters*, *274*, 29–32.
- Barbas, H. (1992). Architecture and cortical connections of the prefrontal cortex in the rhesus monkey. *Advances in Neurology*, *57*, 91–115.
- Beck, A. T., & Steer, R. A. (1987). *Beck depression inventory manual*. San Antonio, TX: The Psychological Corporation.
- Beck, A. T., Ward, C. H., Mendelson, M., Mock, J., & Erbaugh, J. (1961). An inventory for measuring depression. *Archives of General Psychiatry*, *4*, 53–63.
- Bland, B. H., & Oddie, S. D. (1998). Anatomical, electrophysiological and pharmacological studies of ascending brainstem hippocampal synchronizing pathways. *Neuroscience & Biobehavioral Reviews*, *22*, 259–273.
- Borst, J. G., Leung, L. W., & MacFabe, D. F. (1987). Electrical activity of the cingulate cortex. II. Cholinergic modulation. *Brain Research*, *407*, 81–93.
- Botvinick, M. M., Braver, T. S., Barch, D. M., Carter, C. S., & Cohen, J. D. (2001). Conflict monitoring and cognitive control. *Psychological Review*, *108*, 624–652.
- Brett, M., Johnsrude, I. S., & Owen, A. M. (2002). The problem of functional localization in the human brain. *Nature Reviews Neuroscience*, *3*, 243–249.
- Brillinger, D. R. (1981). *Time series: Data analysis and theory*. New York: McGraw-Hill.
- Collins, D. L., Neelin, P., Peters, T. M., & Evans, A. C. (1994). Automatic 3D intersubject registration of MR volumetric data in standardized Talairach space. *Journal of Computer Assisted Tomography*, *18*, 192–205.
- Critchley, H. D., Corfield, D. R., Chandler, M. P., Mathias, C. J., & Dolan, R. J. (2000). Cerebral correlates of autonomic cardiovascular arousal: A functional neuroimaging investigation in humans. *Journal of Physiology*, *523*, 259–270.
- Davidson, R. J., & Irwin, W. (1999). The functional neuroanatomy of emotion and affective style. *Trends in Cognitive Science*, *3*, 11–21.
- Davidson, R. J., Pizzagalli, D., Nitschke, J. B., & Putman, K. (2002). Depression: Perspectives from affective neuroscience. *Annual Review of Psychology*, *53*, 545–574.
- Davis, K. D., Taylor, S. J., Crawley, A. P., Wood, M. L., & Mikulis, D. J. (1997). Functional MRI of pain- and attention-related activations

- in the human cingulate cortex. *Journal of Neurophysiology*, 77, 3370–3380.
- Destra, C., & Ott, T. (1982). Is a retrosplenial (cingulate) pathway involved in the mediation of high frequency hippocampal rhythmical slow activity (theta)? *Brain Research*, 252, 29–37.
- Devinsky, O., Morrell, M. J., & Vogt, B. A. (1995). Contributions of anterior cingulate cortex to behaviour. *Brain*, 118, 279–306.
- Dietl, T., Dirlich, G., Vogl, L., Lechner, C., & Strian, F. (1999). Orienting response and frontal midline theta activity: A somatosensory spectral perturbation study. *Clinical Neurophysiology*, 110, 1204–1209.
- Evans, A. C., Collins, D. L., Mills, S. R., Brown, E. D., Kelly, R. L., & Peters, T. M. (1993). 3D statistical neuroanatomical models from 305 MRI volumes. *Proceedings IEEE Nuclear Science Symposium and Medical Imaging Conference*, 95, 1813–1817.
- Feenstra, B. W., & Holsheimer, J. (1979). Dipole-like neuronal sources of theta rhythm in dorsal hippocampus, dentate gyrus and cingulate cortex of the urethane-anesthetized rat. *Electroencephalography & Clinical Neurophysiology*, 47, 532–538.
- Fisher, R. A. (1921). On the probable error of a coefficient of correlation deduced from a small sample. *Metron*, 1, 3–32.
- Friston, K. J., Worsley, K. J., Frackowiak, R. S. J., Mazziotta, J. C., & Evans, A. C. (1994). Assessing the significance of focal activations using their spatial extent. *Human Brain Mapping*, 1, 214–220.
- Gevins, A., Smith, M. E., McEvoy, L., & Yu, D. (1997). High-resolution EEG mapping of cortical activation related to working memory: Effects of task difficulty, type of processing, and practice. *Cerebral Cortex*, 7, 374–385.
- Hamacher, K., Coenen, H. H., & Stocklin, G. (1986). Efficient stereospecific synthesis of no-carrier-added 2-[18F]-fluoro-2-deoxy-D-glucose using aminopolyether supported nucleophilic substitution. *Journal of Nuclear Medicine*, 27, 235–238.
- Hamilton, M. (1960). A rating scale for depression. *Journal of Neurology, Neurosurgery, and Psychiatry*, 23, 56–62.
- Holsheimer, J. (1982). Generation of theta activity (RSA) in the cingulate cortex of the rat. *Experimental Brain Research*, 47, 309–312.
- Ishii, R., Shinosaki, K., Ukai, S., Inouye, T., Ishihara, T., Yoshimine, T., Hirabuki, N., Asada, H., Kihara, T., Robinson, S. E., & Takeda, M. (1999). Medial prefrontal cortex generates frontal midline theta rhythm. *NeuroReport*, 10, 675–679.
- Jansma, J. M., Ramsey, N. F., Coppola, R., & Kahn, R. S. (2000). Specific versus nonspecific brain activity in a parametric N-back task. *NeuroImage*, 12, 688–697.
- Jueptner, M., & Weiller, C. (1995). Review: Does measurement of regional cerebral blood flow reflect synaptic activity? Implications for PET and fMRI. *NeuroImage*, 2, 148–156.
- Jung, R., & Kornmüller, A. E. (1938). Eine Methodik der Ableitung lokalisierter Potentialschwankungen aus subcorticalen Hirngebieten. *Archiv für Psychiatrie und Nervenkrankheiten*, 109, 1–17.
- Kiehl, K. A., Liddle, P. F., & Hopfinger, J. B. (2000). Error processing and the rostral anterior cingulate: An event-related fMRI study. *Psychophysiology*, 37, 216–223.
- Koski, L., & Paus, T. (2000). Functional connectivity of the anterior cingulate cortex within the human frontal lobe: A brain-mapping meta-analysis. *Experimental Brain Research*, 133, 55–65.
- Kubota, Y., Sato, W., Toichi, M., Murai, T., Okada, T., Hayashi, A., & Sengoku, A. (2001). Frontal midline theta rhythm is correlated with cardiac autonomic activities during the performance of an attention demanding meditation procedure. *Cognitive Brain Research*, 11, 281–287.
- Lancaster, J. L., Rainey, L. H., Summerlin, J. L., Freitas, C. S., Fox, P. T., Evans, A. C., Toga, A. W., & Mazziotta, J. C. (1997). Automated labeling of the human brain—A preliminary report on the development and evaluation of a forward-transformed method. *Human Brain Mapping*, 5, 238–242.
- Leung, L. W., & Borst, J. G. (1987). Electrical activity of the cingulate cortex. I. Generating mechanisms and relations to behavior. *Brain Research*, 407, 68–80.
- Luu, P., Tucker, D. M., Derryberry, D., Reed, M., & Poulsen, C. (2003). Electrophysiological responses to errors and feedback in the process of action regulation. *Psychological Science*, 14, 47–53.
- Magistretti, P. J. (2000). Cellular bases of functional brain imaging: Insights from neuron-glia metabolic coupling. *Brain Research*, 886, 108–112.
- Mayberg, H. S. (1997). Limbic-cortical dysregulation: A proposed model of depression. *The Journal of Neuropsychiatry and Clinical Neurosciences*, 9, 471–481.
- Mayberg, H. S., Brannan, S. K., Mahurin, R. K., Jerabek, P. A., Brickman, J. S., Tekell, J. L., Silva, J. A., McGinnis, S., Glass, T. G., Martin, C. C., & Fox, P. T. (1997). Cingulate function in depression: A potential predictor of treatment response. *NeuroReport*, 8, 1057–1061.
- Meng, X.-L., Rosenthal, R., & Rubin, D. B. (1992). Comparing correlated correlation coefficients. *Psychological Bulletin*, 111, 172–175.
- Milham, M. P., Banich, M. T., Webb, A., Barad, V., Cohen, N. J., Wszalek, T., & Kramer, A. F. (2001). The relative involvement of anterior cingulate and prefrontal cortex in attentional control depends on nature of conflict. *Cognitive Brain Research*, 12, 467–473.
- Murtha, S., Chertkow, H., Beauregard, M., Dixon, R., & Evans, A. (1996). Anticipation causes increased blood flow to the anterior cingulate cortex. *Human Brain Mapping*, 4, 103–112.
- Nunez, P. L., & Silberstein, R. B. (2000). On the relationship of synaptic activity to macroscopic measurements: Does co-registration of EEG with fMRI make sense? *Brain Topography*, 13, 79–96.
- Oakes, T. R., Pizzagalli, D., Hendrick, A. M., Horras, K. A., Larson, C. L., Abercrombie, H. C., Schaefer, S. M., Koger, J. V., & Davidson, R. J. (2001). Simultaneous FDG-PET and 3D tomographic EEG in resting brain. *NeuroImage*, 13, S36.
- Pascual-Marqui, R. D., Lehmann, D., Koenig, T., Kochi, K., Merlo, M. C., Hell, D., & Koukkou, M. (1999). Low resolution brain electromagnetic tomography (LORETA) functional imaging in acute, neuroleptic-naïve, first-episode, productive schizophrenia. *Psychiatry Research: Neuroimaging*, 90, 169–179.
- Pascual-Marqui, R. D., Michel, C. M., & Lehmann, D. (1994). Low resolution electromagnetic tomography: A new method for localizing electrical activity in the brain. *International Journal of Psychophysiology*, 18, 49–65.
- Paus, T. (2001). Primate anterior cingulate cortex: Where motor control, drive and cognition interface. *Nature Reviews Neuroscience*, 2, 417–424.
- Paus, T., Castro-Alamancos, M. A., & Petrides, M. (2001). Cortico-cortical connectivity of the human mid-dorsolateral frontal cortex and its modulation by repetitive transcranial magnetic stimulation. *European Journal of Neuroscience*, 14, 1405–1411.
- Petrides, M., & Pandya, D. N. (1999). Dorsolateral prefrontal cortex: Comparative cytoarchitectonic analysis in the human and the macaque brain and corticocortical connection patterns. *European Journal of Neuroscience*, 11, 1011–1036.
- Phelps, M. E., Huang, S. C., Hoffman, E. J., Selin, C., Sokoloff, L., & Kuhl, D. E. (1979). Tomographic measurement of local cerebral glucose metabolic rate in humans with (F-18)2-fluoro-2-deoxy-D-glucose: Validation of method. *Annals of Neurology*, 6, 371–388.
- Phelps, M. E., Mazziotta, J. C., Kuhl, D. E., Nuwer, M., Packwood, J., Metter, J., & Engel, J., Jr. (1981). Tomographic mapping of human cerebral metabolism visual stimulation and deprivation. *Neurology*, 31, 517–529.
- Pizzagalli, D. A., Nitschke, J. B., Oakes, T. R., Hendrick, A. M., Horras, K. A., Larson, C. L., Abercrombie, H. C., Schaefer, S. M., Koger, J. V., Benca, R. M., Pascual-Marqui, R. D., & Davidson, R. J. (2002). Brain electrical tomography in depression: The importance of symptom severity, anxiety, and melancholic features. *Biological Psychiatry*, 52, 73–85.
- Pizzagalli, D., Pascual-Marqui, R. D., Nitschke, J. B., Oakes, T. R., Larson, C. L., Abercrombie, H. C., Schaefer, S. M., Koger, J. V., Benca, R. M., & Davidson, R. J. (2001). Anterior cingulate activity as a predictor of degree of treatment response in major depression: Evidence from brain electrical tomography analysis. *American Journal of Psychiatry*, 158, 405–415.
- Rosenthal, R. (1987). *Judgment studies: Design, analysis, and meta-analysis*. New York: Cambridge University Press.
- Sasaki, K., Nambu, A., Tsujimoto, T., Matsuzaki, R., Kyuhou, S., & Gemba, H. (1996). Studies on integrative functions of the human frontal association cortex with MEG. *Cognitive Brain Research*, 5, 165–174.
- Schacter, D. L. (1977). EEG theta waves and psychological phenomena: A review and analysis. *Biological Psychology*, 5, 47–82.
- Sokoloff, L. (1989). Circulation and energy metabolism of the brain. In G. J. Siegel, B. W. Agranoff, R. W. Albers, & P. B. Molinoff (Eds.),

- Basic neurochemistry: Molecular, cellular, and medical aspects* (4th ed., pp. 565–590). New York: Raven Press.
- Sokoloff, L., Reivich, M., Kennedy, C., Des Rosier, M. H., Patlak, C. S., Pettigrew, K. D., Sakurada, O., & Shinohara, M. (1977). The [¹⁴C]deoxyglucose method for the measurement of local cerebral glucose utilization: Theory, procedure and normal values in the conscious and anesthetized albino rat. *Journal of Neurochemistry*, *28*, 897–916.
- Spitzer, R. L., Williams, J. B. W., Gibbon, M., & First, M. B. (1992). *Structured Clinical Interview for DSM-III-R*. Washington, DC: American Psychiatric Press.
- Steriade, M., Gloor, P., Llinás, R. R., Lopes da Silva, F. H., & Mesulam, M. M. (1990). Report of IFCN Committee on Basic Mechanisms. Basic mechanisms of cerebral rhythmic activities. *Electroencephalography & Clinical Neurophysiology*, *76*, 481–508.
- Swanson, L. W., & Cowan, W. M. (1979). The connections of the septal region in the rat. *Comparative Neurology*, *186*, 621–656.
- Talairach, J., Bancaud, J., Geier, S., Bordas-Ferrer, M., Bonis, A., Szikla, G., & Rusu, M. (1973). The cingulate gyrus and human behaviour. *Electroencephalography & Clinical Neurophysiology*, *34*, 45–52.
- Talairach, J., & Tournoux, P. (1988). *Co-planar stereotaxic atlas of the human brain*. New York: Thieme Medical Publishers, Inc.
- Tesche, C. D., & Karhu, J. (2000). Theta oscillations index human hippocampal activation during a working memory task. *Proceedings of the National Academy of Sciences, USA*, *97*, 919–924.
- Tomarken, A. J., Davidson, R. J., Wheeler, R. W., & Kinney L. (1992). Psychometric properties of resting anterior EEG asymmetry: Temporal stability and internal consistency. *Psychophysiology*, *29*, 576–592.
- Towle, V. L., Bolanos, J., Suarez, D., Tan, K., Grzeszczuk, R., Levin, D. N., Cakmur, R., Frank, S. A., & Spire, J. P. (1993). The spatial location of EEG electrodes: Locating the best-fitting sphere relative to cortical anatomy. *Electroencephalography & Clinical Neurophysiology*, *86*, 1–6.
- Vertes, R. P., & Kocsis, B. (1997). Brainstem-diencephalo-septohippocampal systems controlling the theta rhythm of the hippocampus. *Neuroscience*, *81*, 893–926.
- Vinogradova, O. S. (1995). Expression, control, and probable functional significance of the neuronal theta-rhythm. *Progress in Neurobiology*, *45*, 523–583.
- Williams, L. M., Brammer, M. J., Skerrett, D., Lagopoulos, J., Rennie, C., Kozek, K., Olivieri, G., Peduto, T., & Gordon, E. (2000). The neural correlates of orienting: An integration of fMRI and skin conductance orienting response. *NeuroReport*, *11*, 1–5.

(RECEIVED March 28, 2002; ACCEPTED May 27, 2003)